

Particle Fluctuations in Ion Channels

AMSURE 2021

Johanna McCombs

Advisors: Sophie Marbach and Brennan Sprinkle

Abstract

Individual ions undergo random motion and pass through ion channels arranged in the cell membrane. Statistical measurements are difficult to calculate in an individual channel, consequently making it difficult to understand these processes. Here we investigate the number of ions in a channel by simulating the random particle movement through an arbitrary channel, and calculating the mean squared displacement, to expand on previous work. The previous model agrees with the simulated data in a one dimensional case, but in a two dimensional case the simulated data deviates from the previous theoretical model. From our simulations we modified the previous model to agree to simulated data for short times. This advancement provides a starting point for further research with different particle conditions or a three-dimensional setting.

1 Introduction

On a molecular level particles diffuse from an area of high concentration to low concentrations. This diffusion process is partially a result of Brownian motion. Brownian motion occurs when small granules or particles are bombarded by surrounding atoms undergoing thermal movements [2]. These smaller molecules provide both the damping, which restricts vibratory motion, and driving forces, which provide energy to the particles on a microscopic level. These forces create a random motion of specific particles called ions, examples of which are potassium, sodium and calcium [2]. The liquid that contains these molecules and particles is found surrounding cell membranes. Cell membranes contain proteins, called ion channels, that arrange to allow passage for particles from one side of the membrane to the other. While these particles pass through the pore they still undergo random motion [4]. Pore size can determine the permeability of water and rejection of other solutes [6]. There is limited understanding of how these ions behave passing through these channels because of the difficulty to make statistical measurements of a single particle.

1.1 Brownian Motion

Here we present Brownian motion.

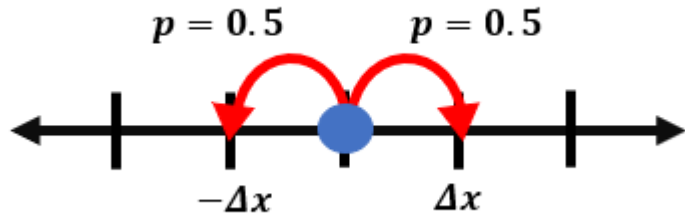


Figure 1: Diagram of a particle (blue circle) moving on a one dimensional line with equal probability (p) of moving left or right

In a one dimensional setting the particle begins at the origin and at each time step(τ) has equal probability of moving the same distance left or right on a line, creating a discrete random walk [5]. When τ becomes very small, this discrete walk becomes continuous. Eq.(1) shows the probability of finding the particle at position x at time t .

$$p(x, t) = \frac{1}{\sqrt{2\pi Dt}} e^{\frac{-x^2}{2Dt}} \quad (1)$$

where D is the diffusion coefficient. Eq.(1) satisfies the Fokker-Planck equation $\frac{\partial p}{\partial t} = D \frac{\partial^2 p}{\partial x^2}$. A stochastic process, known as the Wiener process can further describe Brownian motion. The Wiener Process is the limit of a discrete random walk with very small steps, and described by Eq.(2), where X_k is the particle's position at time k and W_k is Gaussian white noise[1].

$$\Delta X_k = X_{k+1} - X_k = D W_{k\tau} = \sqrt{2D\tau} W_k \quad (2)$$

In the simulations described below we use (3) to describe the motion of the particles. The process above can be equivalently described by the Langevin equation below[1].

$$\zeta v(t) = \sqrt{\frac{2k_B T \zeta}{\Delta t}} W \quad (3)$$

$$\frac{X_k(t + \Delta t) - X_k(t)}{\Delta t} = v(t) \quad (4)$$

where $x(t)$ is particle position x at time t , ζ is the friction coefficient, k_B is Boltzmann constant, T is temperature, Δt is the time increment and W is a normally distributed random variable. The mean of W denoted by $\langle W \rangle = 0$, and the variance denoted by $\langle W(t)W(t') \rangle = \delta(t - t')$. Here $\langle \dots \rangle$ is the average over realizations of the noise. These equations can be extended to 2D by calculating Eq.(3) with two different random variables (W_x and W_y) for x and y for each of the axes. Using a 2D setting more accurately shows how a particle moves in a real space. In this space, the introduction of other components such as artificial channels provides an even better understanding of particle behavior, which is what I looked at in this project.

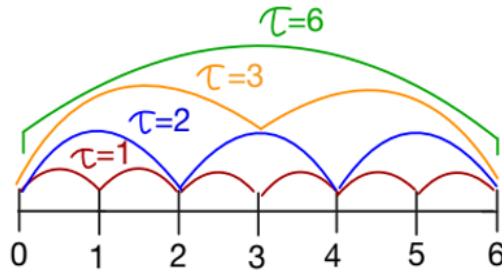
The mean $\langle x(t) \rangle$ gives limited information. To better understand the particle behavior and trajectory we use the statistical method of taking the mean squared displacement(MSD).

1.2 Mean Squared Displacement (MSD)

Mean squared displacement is the sum of the squared deviation of the position of a particle from a reference position over times[1], shown in Eq. (5).

$$MSD(\tau) = \langle \Delta x(\tau)^2 \rangle = \langle [x(t + \tau) - x(t)]^2 \rangle \quad (5)$$

To obtain more data for one particle trajectory, various values of t are used, from 1 to τ , τ being the total time the trajectory is tracked. For example, if $\tau = 1$ with Δt the MSD is calculated between every position, or if $\tau = 2$ then the MSD is calculated between every other position which is shown in the sketch below where it starts at $t = 0$. It would then start at $t = 1$ and increase by τ .



Standard Brownian motion has a linear MSD as the particle moves in time. Below, the derivation of the MSD of standard Brownian motion is done. Starting from Eq. (3) and (4),

$$\begin{aligned}
\zeta v(t) &= \sqrt{\frac{2k_B T \zeta}{\Delta t}} W & v(t) &= \frac{X_k(t + dt) - X_k(t)}{\Delta t} \\
\zeta \frac{X_k(t + dt) - X_k(t)}{\Delta t} &= \sqrt{2k_B T \zeta} W \\
X_k(t + \Delta t) - X_k(t) &= \frac{1}{\zeta} \Delta t \sqrt{2k_B T \zeta} W \\
\langle (X_k(t + \Delta t) - X_k(t))^2 \rangle &= \left\langle \frac{1}{\zeta} \Delta t \sqrt{2k_B T \zeta} W \right\rangle^2 \\
\langle (X_k(t + \Delta t) - X_k(t))^2 \rangle &= \frac{2k_b T}{\zeta} \Delta t \langle W^2 \rangle \\
\langle (X_k(t + \Delta t) - X_k(t))^2 \rangle &= \frac{2k_b T}{\zeta} \Delta t
\end{aligned}$$

If the motion happens in many dimensions the MSD of a particle trajectory, where d is dimension, is,

$$\langle \Delta X_k(\Delta t)^2 \rangle = \frac{2k_B T d}{\zeta} \Delta t. \quad (6)$$

Now, instead of looking at standard Brownian motion, we can look at Brownian motion with an added ion channel, not considering the surrounding membrane. An imaginary box is defined to represent the real channel. At each time step the amount of particles inside the imaginary box, representing particles passing through the channel, can be counted and called N . This is shown in Fig.2. When the MSD is taken of the number of particles in the channel it is not linear, unlike the MSD of standard Brownian motion. The theoretical expression for this MSD calculation derived from counting particles coming in and out of the box is below in the case of an infinitely long rectangle [3].

$$\langle (N(t + t_0) - N(t_0))^2 \rangle = 2N_0 \left[\left(1 - e^{\frac{-w^2}{4Dt}} \right) \sqrt{\frac{4Dt}{\pi w^2}} + 1 - \text{erf} \left(\frac{w}{\sqrt{4Dt}} \right) \right] \quad (7)$$

$N(t)$ is the number of particles within the channel, N_0 is the average number of particles in the channel, and w is the width of the channel, which will be further explained in Section 2. This expression describes the MSD for number of particles in the channel in one dimension or when the width(w) approaches 0 and the height(h) of the channel approaches ∞ . When the general shape of the channel becomes more square or $h=w$ the theoretical expression does not properly describe the MSD of number of particles in the channel. The goal of this paper is to explore how to adjust the theoretical equation in Eq.(7) to more accurately describe the MSD of number of particles in the arbitrary channel over a period of time.

2 Simulations

2.1 Simulation Set Up

To model particles undergoing Brownian motion and passing through ion channels, we first started with simulating multiple particle trajectories in a custom made MATLAB rou-

tine. These trajectories were created using Eq.(3) and Eq.(4) in Section 1.1. Each particles position on the x and y was recorded at each time step. In all simulations set parameter values were chosen as $k_B T = 0.004$ and $\zeta = 6\pi(0.001)$ resulting in $D = \frac{k_B}{\zeta} \approx 0.222 \times \frac{l^2}{\Delta t}$, where l an arbitrary unit length. The random variable W was determined using MATLAB's random normally distributed number generator. To obtain enough data to plot smooth data at early times the particles trajectories were ran for at least time $T = 200000 \Delta t$ ($\Delta t = 1$).

In a lab setting particles pass through the observed region and leave the observed region. To simulate this movement and create "new" particles we used periodic boundary conditions. This region was defined by it's height, h , and width, w , and centered around the origin. When the particle trajectories were generated and if the particle's position was outside of the region, the particle would be placed on the opposite side of it's exit position in the region an equal distance to which it left the region. Consistently throughout the simulations the width was $200l$, with the height an equivalent length, with 2000 particles. A sufficiently large periodic box ensures that the MSD will not be affected at long times. The particles at time zero were placed randomly in the periodic box.

Within the periodic bounded region an artificial box was made defined by height h and width w . This box represents the ion channel which the particles pass through. In these simulation the surrounding membrane is not considered. Rather than track each individuals particle's movement through the box, at each time step in t the number of particles in the box, $N(t)$, was counted. Box sizes varied, we commonly looked at box ratios($\frac{h}{w}$) of 1 to 20, where 1 is a square box, and 20 is a rectangular box spanning the height of the periodic box.

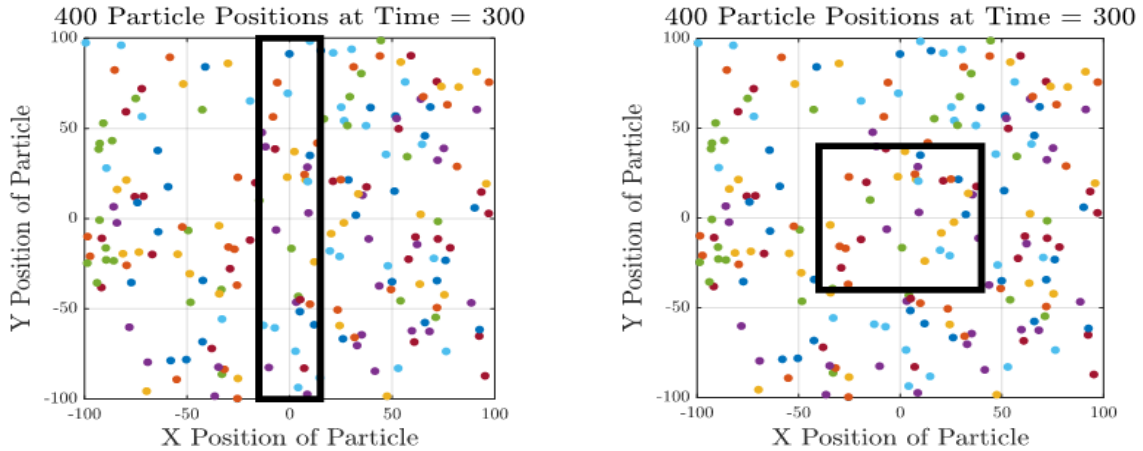


Figure 2: Example of particle positions in the periodic bounded region with different box sizes at time 300

We calculated the MSD of $N(t)$ for different box height to width ratios ($\frac{h}{w}$). To calculate the MSD for each value of τ to the maximum increment value(T), we calculated $\sum_{t=0}^{T-\tau} (N(t + \tau) - N(t))^2$, then divided by t/τ . Then divided by the average number of particles in the box over T . The result is an array from 1 to τ , with the MSD corresponding to the value of τ or "inc" in the code below.

```

function [MSD] = MSDcalc(NumofPart,averageNum,stopt)
%MSD for short time
%NumofPart- N(t)
%averageNum - N(t) / (total number of particles)
%stopt - max increment size
arrayPos=1;
sum = 0;
time=length(NumofPart);
MSD= zeros(1,stopt);
for inc =1:stopt
for pos = 1:time-inc
difsqr=(NumofPartt(c+pos)-NumofPart(pos))^2;
sum = sum + difsqr;
end
M = sum/ (time-inc);
MSD(z)= M/averageNum;
sum = 0;
arrayPos= arrayPos +1;
end
end

```

Figure 3: Sample of code to calculate the MSD in MATLAB

2.2 Theoretical MSD

Figure 4 shows data obtained from the simulations of MSD of number of particles in the box plotted against the theoretical curve shown in Eq.(7) for MSD. For a ratio($\frac{h}{w}$) of 20 a rectangle the simulations agreed with the theoretical Eq.(7) for short and long times. As the ratio becomes square Eq.(7) increasingly deviates from the simulated data.

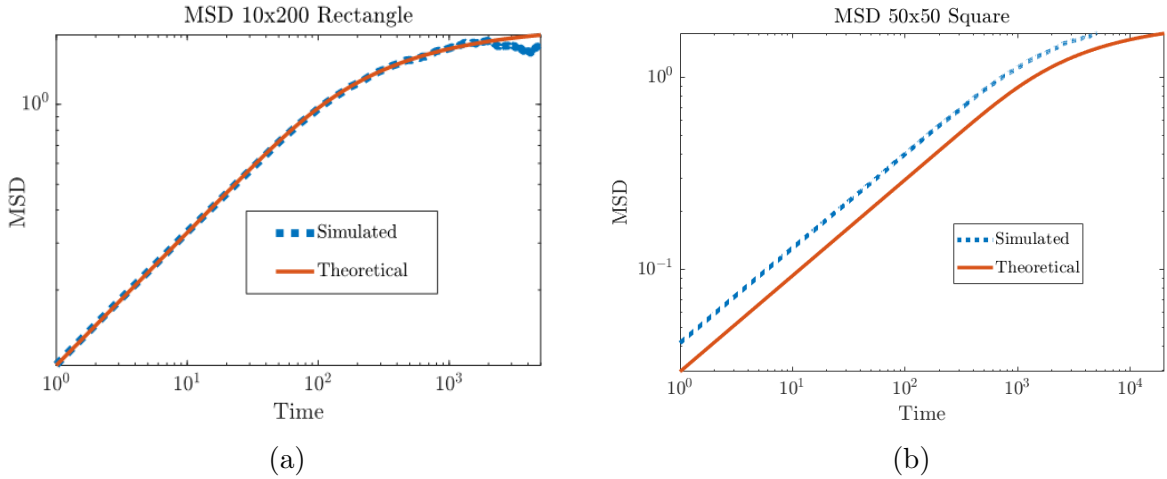


Figure 4: Comparison of MSD of simulated data to theoretical MSD Eq. (7). $\Delta t = 1$ and $t=500000$.

We focused on discrepancies at early times. From Eq.(7), $2N_0\sqrt{\frac{4Dt}{\pi w^2}}$ describes the behavior of the MSD in early times. To test where the theoretical MSD deviated from the simulated data, the simulated data of MSD at early times was fitted to the power function $b \cdot t^a$ for different box height to width ratios($\frac{h}{w}$), where w was kept at $w = 10$. Theoretically $b = 2\sqrt{\frac{4D}{\pi w^2}}$ and $a = 0.5$.

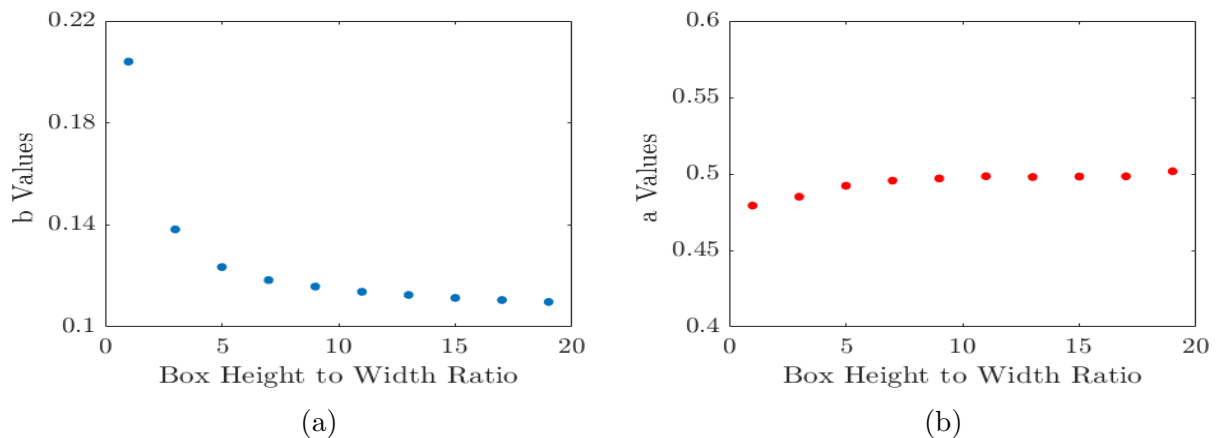


Figure 5: Values of a and b from simulated MSD data at early times ($t=50000$) fitted to bt^a for different values of $\frac{h}{w}$

Figure 5a indicates the values of b are not consistent with the expected theoretical values, which should be approximately 0.1 for all values of $\frac{h}{w}$. Values of a in Fig. stays consistent with the expected values of about 0.5. To further understand the simulated vs. theoretical value of b , the data in Figure 3.a was fitted to the power function $c \left(\frac{h}{w}\right)^d + g$

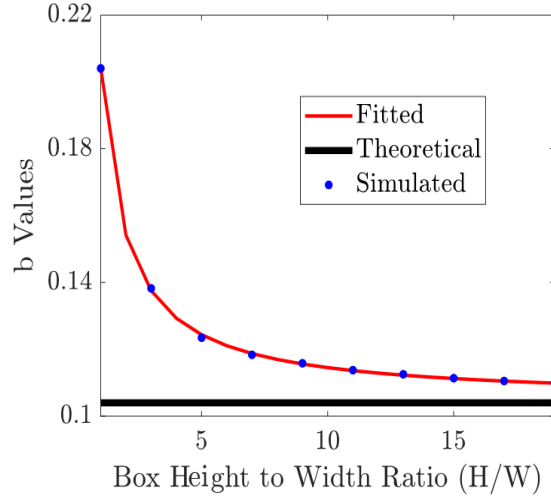


Figure 6: Simulated values of b fitted to $c \left(\frac{h}{w}\right)^d + g$ and compared to the expected theoretical value

The values of c, d , and g were found to be $c = g = 2\sqrt{\frac{4D}{\pi w^2}}$ which will now be referred to as b_∞ and $d \approx -1$. Using these an adjusted theoretical value of b is found.

$$b\left(\frac{w}{h}\right) = b_\infty \frac{w+h}{h} = \frac{2\sqrt{4D}}{h} \left(\frac{w+h}{h}\right)$$

Let $R = \frac{wh}{h+w}$. Now, introducing this value of R in place of w , and adding factor of 2 to account for two dimensions(dimensional component seen in Eq. (6)) in Eq. (7), we obtain,

$$\langle (N(t+t_0) - N(t_0))^2 \rangle = 2N_0 \left[\left(1 - e^{\frac{-R^2}{8Dt}}\right) \sqrt{\frac{8Dt}{2\pi R^2}} + 1 - \text{erf}\left(\frac{R}{\sqrt{8Dt}}\right) \right]. \quad (8)$$

Figure 7 compares simulated data for the MSD and Eq.(8) to determine if this adjusted theoretical prediction represents simulated data better for more square box height to width ratios. Fig.8 shows the comparison of MSD for longer times. This comparison will be discussed in the next section.

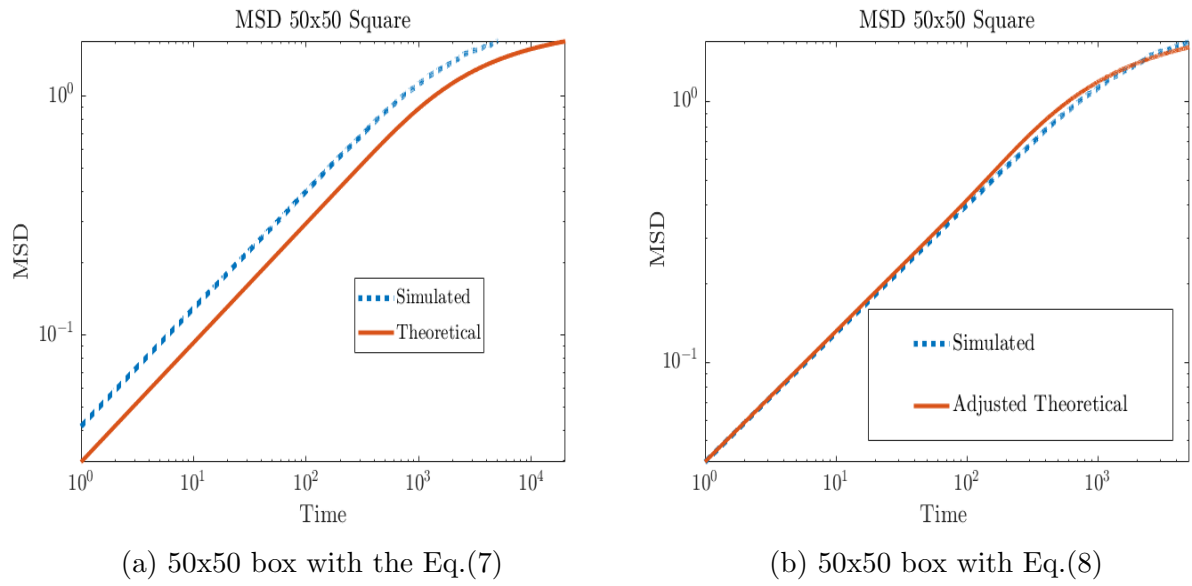


Figure 7: Comparison of Eq. (7) and Eq. (8) against simulated MSD

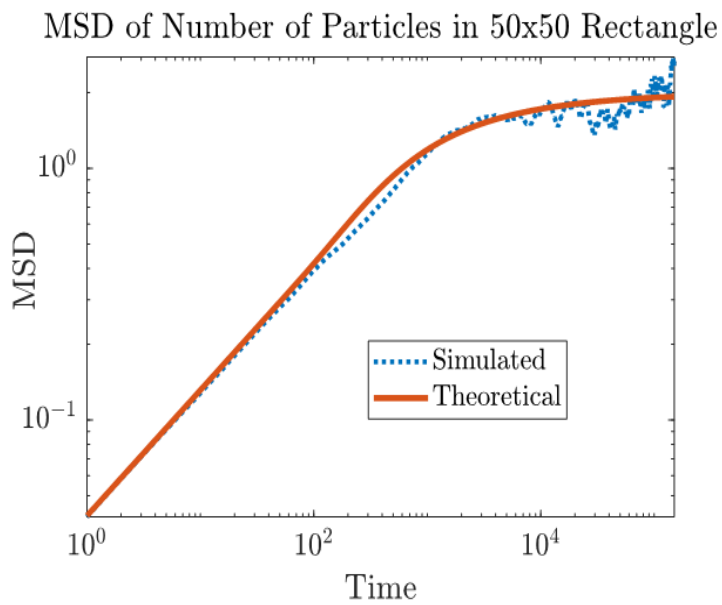


Figure 8: Equation 8 shown for long times

3 Discussion and Conclusion

As seen in Fig.7 the adjusted theoretical(Eq.(8) agrees with the simulated data for short times with visible improvement from Eq. (7). From time $t = 0$ to $t = 10^2$ the adjusted theoretical is the most accurate, then around $t = 10^3$ there is a small deviation from the simulated data. This deviation is more visible in Fig. 8 when Eq.(8) is plotted for longer times but the adjusted theoretical still follows the general trend of the simulated data. After $t = 10^4$ the simulated data has a large amount of statistical error. Obtaining enough data to limit statistical error is difficult at long time periods because it requires large computing resources. To test the agreement of Eq.(8) with simulated data for long times, smoother data is needed. Then to further adjust the original theoretical expression(Eq.(7)) the proper modifications need to be found for the long time data. An analytic derivation of the new value of b is also needed to demonstrate that the simulated value found is correct.

This project only focused on a small portion of the bigger picture of how particles behave in and around ion channels. Understanding this setting requires looking at many different components with small differences. Here we looked at one of the simpler cases with a rectangular channel, with limited particle conditions, this work could easily be expanded to introduce new restrictions and provide added accuracy to the model.

In all simulations the particles had size zero. To further investigate how particles behave inside ion channels, altering particle size to a finite size would provide further insights. With finite size there would be a maximum number of particles allowed in the ion channel at once instead of infinitely many particles.

Another restriction could be boundaries for the membrane, which would restrict the movement of the particles and how they an pass through the artificial channel. In addition to particle size the density of number of particles with finite size would affect the dynamics because the particles would hit each other more frequently. These factors should all be considered when moving forward with this researcht.

References

- [1] B. I. Henry, T. a. M. Langlands, and P. Straka. “An Introduction to Fractional Diffusion”. In: *Complex Physical, Biophysical and Econophysical Systems*. Vol. Volume 9. World Scientific Lecture Notes in Complex Systems Volume 9. WORLD SCIENTIFIC, Mar. 1, 2010, pp. 37–89. ISBN: 978-981-4277-31-0.
- [2] M.H. Holmes. *Introduction to the Foundations of Applied Mathematics*. Texts in Applied Mathematics. Springer New York, 2009, ISBN: 978-0-387-87749-5.
- [3] S. Marbach. “Intrinsic fractional noise in nanopores: The effect of reservoirs”. In: *The Journal of Chemical Physics* 154.17 (May 7, 2021). Publisher: American Institute of Physics, p. 171101. ISSN: 0021-9606.
- [4] Mark S. P. Sansom et al. “Simulations of ion channels – watching ions and water move”. In: *Trends in Biochemical Sciences* 25.8 (Aug. 1, 2000). Publisher: Elsevier, pp. 368–374. ISSN: 0968-0004.
- [5] Charles J. Weiss. “Introduction to Stochastic Simulations for Chemical and Physical Processes: Principles and Applications”. In: *Journal of Chemical Education* 94.12 (Dec. 12, 2017). Publisher: American Chemical Society, pp. 1904–1910. ISSN: 0021-9584.
- [6] Jay R. Werber, Chinedum O. Osuji, and Menachem Elimelech. “Materials for next-generation desalination and water purification membranes”. In: *Nature Reviews Materials* 1.5 (May 2016), p. 16018. ISSN: 2058-8437.